Journal of Electromyography and Kinesiology 70 (2023) 102774

Contents lists available at ScienceDirect

Journal of Electromyography and Kinesiology

journal homepage: www.elsevier.com/locate/jelekin

Review

Skeletal muscle models composed of motor units: A review

Rositsa Raikova [a,*], Piotr Krutki [b], Jan Celichowski [b]

[a] Institute of Biophysics and Biomedical Engineering, Bulgarian Academy of Sciences, Bulgaria
[b] Department of Neurobiology, Poznan University of Physical Education, Poland

ARTICLE INFO

Keywords:
Twitch model
Tetanus
Decomposition
Recruitment
Muscle force

ABSTRACT

The mathematical muscle models should include several aspects of muscle structure and physiology. First, muscle force is the sum of forces of multiple motor units (MUs), which have different contractile properties and play different roles in generating muscle force. Second, whole muscle activity is an effect of net excitatory inputs to a pool of motoneurons innervating the muscle, which have different excitability, influencing MU recruitment. In this review, we compare various methods for modeling MU twitch and tetanic forces and then discuss muscle models composed of different MU types and number. We first present four different analytical functions used for twitch modeling and show limitations related to the number of twitch describing parameters. We also show that a nonlinear summation of twitches should be considered in modeling tetanic contractions. We then compare different muscle models, most of which are variations of Fuglevand's model, adopting a common drive hypothesis and the size principle. We pay attention to integrating previously developed models into a consensus model based on physiological data from *in vivo* experiments on the rat medial gastrocnemius muscle and its respective motoneurons. Finally, we discuss the shortcomings of existing models and potential applications for studying MU synchronization, potentiation, and fatigue.

1. Introduction

The primary physiological function of skeletal muscles is contraction, allowing the body to maintain posture and move. Each muscle is innervated by a set of motoneurons and each of them innervates group of muscle fibers dispersed within the muscle. The motoneuron, its axon, and respective group of muscle fibers form the smallest functional unit, the motor unit (MU). Therefore, realistic modeling of muscle functions should be based on knowledge of muscle structure and physiology, and simulate motoneuron activity and the force generated by MUs recruited into mechanical action. Such an approach is a progression from Hill-type models (Zajac, 1989; Brown et al., 1999), representing the muscle as a combination of contractile and elastic elements with an input (activation signal) to the whole muscle. In modeling the muscle force, taking into account the participation of individual MUs, there are two different approaches. The first are the predictive muscle models, predominantly based on the classic model of Fuglevand et al. (1993), using a relatively simple MU twitch model, applied to simulate consequences of changes in the firing rate and recruitment for the muscle output force and/or electromyogram (Williams and Baker, 2009; Johnston et al., 2010; Nagamori et al., 2021). The factors underlying saturation of motoneuronal firing rate in human muscle were also studied using this approach (Fuglevand et al., 2015). Considerable progress in modeling muscle force of human triceps surae (medial gastrocnemius, lateral gastrocnemius and soleus) was achieved by the Brazilian group in their impressive studies on models of neurons, muscle proprioceptors and elements of body biomechanics during upright stance (Elias and Kohn, 2013; Elias et al., 2012, 2014; Watanabe et al., 2013). Interestingly, they included into the modeling differentiation of MUs into three basic types: S, FR and FF (Watanabe et al., 2013). The second approach to modeling of muscle force is reflected in the descriptive studies, predominantly focused on as accurate as possible description of the MU twitch, changes of its properties, the summation into tetanic contractions, and finally simulation of the muscle force, being a result of summation of forces generated by individual MUs (Celichowski et al. 2014; Raikova et al., 2007a, 2008, 2013, 2016b, 2018, 2021).

This review predominantly summarizes advances and challenges in descriptive modeling of skeletal muscle force based on the physiological knowledge of motoneuron activity and the production of force by MUs. In such modeling, two issues are crucial from the mechanical perspective: a precise model of the twitch (the mechanical MU's response to one action potential of a motoneuron) and realistic models of tetanic

* Corresponding author.
E-mail address: rosi.raikova@biomed.bas.bg (R. Raikova).

https://doi.org/10.1016/j.jelekin.2023.102774
Received 28 November 2022; Received in revised form 6 April 2023; Accepted 9 April 2023
Available online 19 April 2023

contractions (responses to a series of action potentials resulting in the summation of twitches). Moreover, at least two mechanisms of force regulation should be considered: the recruitment and decruitment of different MU types during muscle contraction and the rate coding (i.e., regulation of active MU forces by changes in the frequencies of action potentials generated by motoneurons). In the first part of this review, we discuss the modeling of MU forces and present methods for calculations of twitches and tetanic contractions. In the second part, we will focus on rat medial gastrocnemius model composed of three MUs types and consequencies of their recruitment and decruitment.

2. MU diversity

For mammalian hind limb muscles, the MU population can be divided into three separate physiological types whose contractile properties are considerably different (Burke et al., 1973): slow-twitch (S), fast-twitch resistant to fatigue (FR), and fast-twitch fatigable (FF), responsible for antigrativy contractions, walking and running, respectively. For different types of MUs in rat hind limb muscles distinct differences in their daily activity were documented (Hennig and Lømo, 1985). Nevertheless, it should be stressed that in humans most frequently upper limb muscles were studied, and the three clusters of MUs are not evident (Bigland-Ritchie et al., 1998, for review see Heckman and Enoka, 2012), which seems to correspond to a large spectum of their activities. S MUs typically have the lowest force, longest twitch, and highest fatigue resistance, while FF MUs are the strongest and most fatigable. Moreover, the number of muscle fibers innervated by one motoneuron (the innervation ratio) is the primary determinant of the force generated by a MU, which is lowest for S and highest for FF MUs (Burke, 1981). S MUs are the first activated during muscle contraction, whereas FF MUs are the last, and only during strong and rapid contractions. This recruitment order is often referred to as "the size principle" (Henneman, 1957) since it relates to the size and excitability of motoneurons: the smallest and the most excitable are S motoneurons, and the largest and the least excitable are FF motoneurons. Therefore, it is necessary to include motoneuron properties to muscle modeling. The probability of motoneuron excitation depends on their input resistance, the rheobase, and the depolarization threshold (Zengel et al., 1985). However, the recruitment depends also on the effective synaptic current activating motoneurons, which is not uniform among low and high-threshold motoneurons (Powers and Binder, 2001). Moreover, motoneuron discharge frequencies during prolonged activity are considerably lower for slow than fast MUs (Kernell, 1979; Krutki et al., 2015). For all MU types, the minimum discharge frequency of motoneurons is sufficient to induce a tetanic contraction of relatively low force in muscle fibers of the innervated MU. In contrast, the maximum frequencies correspond to tetanic contractions reaching 80–95% of maximal MU force (Kernell, 1965).

One should note that considerably different firing bahaviours can be observed in various mammalian muscles. During voluntary activity fast and slow MUs in rat hind limb muscles show evidently different firing rates. Hennig and Lømo (1985) revealed that the mean firing rates were 18–21 Hz for slow MUs in the soleus muscle, whereas 48–91 Hz for fast MUs in the extensor digitorum longus muscle. These frequencies were related to the twitch contraction times in respective rat muscles and corresponded to the steep parts of the force-frequency relationships (reflecting the ability for summation into unfused tetanic contractions). On the other hand, the "onion skin" behaviour was observed in isometric contractions of human muscles (at moderate levels of force low threshold MUs fire at higher rates that those recruited lately) (De Luca and Erim, 1994). Such behaviour was predominantly reported for muscles of upper limbs, for which the spectrum of motor activities is wider and MUs are not clustered into three categories. On the contrary, in human lower limb muscles (see Garnett et al. 1979 for data on medial gastrocnemius) MUs form three separate clusters (S, FR and FF), responsible for standing, walking, and running, respectively, similarly as in animal hind limb muscles. These inconsistencies between muscle types and between different species are challenging for muscle modeling since a general model should either contain simplifications or will be unsuitable for all muscles.

Reliable muscle models should reflect MU diversity and composition within a given muscle since they differ considerably in the number and proportions of particular MU types. For example, the rat medial gastrocnemius muscle is composed of three MU types, predominantly FF and FR (Krutki et al., 2006), while the soleus muscle, which acts similarly on the ankle joint, contains almost exclusively S MUs (Drzymała-Celichowska et al., 2012).

3. MU twitch modeling

The simplest MU contraction is the twitch, a response to a single action potential of a motoneuron. The MU twitch is characterized by an "all-or-none" appearance since all muscle fibers innervated by a motoneuron are synchronously activated via neuromuscular junctions. In classical electrophysiological experiments the twitch is recorded as a response to single activation of the axon of a motoneuron (the MU twitch) or the nerve (the muscle twitch). This method of a single MU activation is applied predominantly in animal research whereas in human experiments the spike triggered averaging technique is used (Thomas et al., 1987; Roatta et al., 2008; Negro and Orizio, 2017). This impressive technique enables an estimation of the twitch waveform of single MUs *in vivo* by averaging the joint force signal from numerous MU action potentials. The force signal is usually recorded during the muscle voluntary activity at a relatively low level of force. However, this method has several limitations. First of all a record obtained with this technique is a twitch-shape fragment of an unfused tetanic contraction, and its duration and amplitude are sensitive to the fusion degree of this tetanus, because they depend on a duration of a preceeding interpulse interval between MU action potentials (Nordstrom et al., 1989; Negro et al., 2014; Dideriksen and Negro, 2018). Nevertheless, the observations based on spike triggered averaging technique drew attention to a fact that responses to successive action potentials of motoneurons may be significantly different.

The twitch force course recorded under isometric conditions has a bell-shaped form consisting of two phases: the force increase up to the peak, known as the contraction time, and the relaxation phase when the force decreases exponentially back to baseline. The course of the second phase is most often described by a half-relaxation time parameter (when the decreasing force reaches half its maximal value) due to frequent difficulties in determining the precise end of relaxation. The twitch model includes a short delay representing the time between the stimulus and the beginning of the force recording, reflecting the conduction of an action potential along the motor axon, its transmission by the neuromuscular junction to muscle fibers, and the activation of the contractile apparatus in sarcomeres.

A mathematical twitch model is a primary challenge in modeling MU force since it introduces the possibility of simulating unfused tetanus in which many twitches are summed according to the patterns of action potentials. Several studies proposed various approaches to this problem. Fig. 1 shows a sample twitch induced by the electrical stimulation of a motoneuron axon recorded in an electrophysiological experiment and indicates the common twitch parameters included in the most popular models to compare different analytical forms used for describing the twitch. The plotted curve has several specific points: the start of the contraction, the moment where the force reaches its maximum, and two points where the force reaches half of its maximal value. Moreover, the twitch does not start at zero time but at the moment ($T_{imp} + T_{lead}$). Different values of these specific points characterize twitches experimentally recorded during contractions of different MU types (S, FR, and FF), and several analytical functions were used to describe the twitch.

The simplest analytical formula describing a force developed in response to an action potential was proposed by Milner-Brown et al.

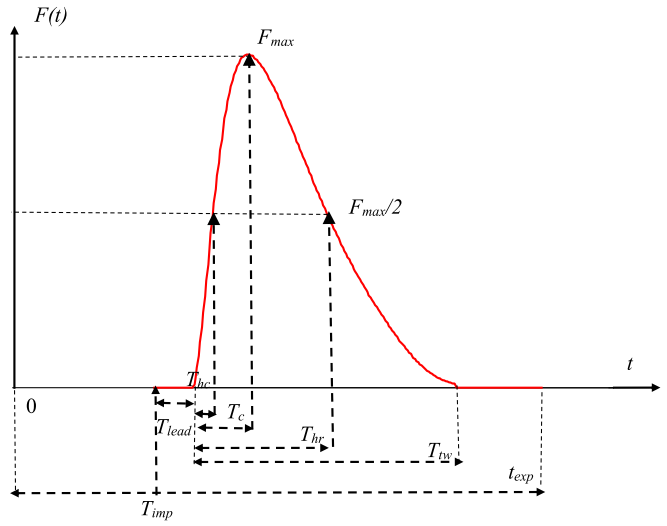

Fig. 1. Parameters of the twitch model in a function of MU force time *F(t)*. F_{max}, the maximal force; T_{imp}, the time moment of the action potential; T_{lead}, the lead time (time between the action potential and the start of force development); T_c, the contraction time (time between the start of force development and the moment when the force reaches its maximum; T_{hc}, the half-contraction time (time between the start of the contraction and the moment when the force reaches half of its maximum); T_{hr}, the half-relaxation time (time between the start of the mechanical response and the moment during relaxation period when the force reaches half of its maximum); T_{tw}, the time between the start and the end of the contraction (defined as the time when MU force decreases to $F_{max}/1000$); t_{exp}, the experiment time (force is zero from $t = 0$ to $t = T_{imp}$ and from $t = T_{tw}$ to $t = t_{exp}$).

(1973). They modeled twitch force as a response of a critically damped second-order system, and the twitch delay (T_{lead}) was ignored (see the Appendix in Milner-Brown et al., 1973). The proposed function accounted only for the contraction time and the maximal twitch force (the peak tension). The half relaxation time (T_{hr}) was strongly associated with the contraction time (T_c) and this relation was set at $\approx 2.68T_c$, so the relaxation phase of the twitch could not be independently controlled. This formula was later ameliorated and applied by Fuglevand et al. (1993) who proposed the largely accepted model of muscle containing a pool of 120 individually driven MUs. The twitch amplitude of these MUs substantially varied within the range based on experimental data.

In 1982, Piotrkiewicz published another form of the twitch force, called a mechanogram, which was also an impulse response to a linear, second-order system near critical damping (Piotrkiewicz, 1982). As in the previous example, the parameters considered were only T_c and F_{max}, with the formula:

$$F_{twPiot}(t) = F_{\max}\frac{t}{T_c}\exp\left(0.5\left(1-\frac{t^{\wedge 2}}{T_c}\right)\right) \quad (1)$$

where $F_{twPiot}(t)$ is the MU force as a function of time *t*. It should be noted that the true time for each twitch with impulse (corresponding to a motoneuron action potential) in time T_{imp} was:

$$tau(t) = t + T_{lead} + T_{imp} \quad (2)$$

An inequality constraint was also imposed, such that if $F_{twPiot}(t) < F_{\max}/1000$, then $F_{twPiot}(t) = 0$.

Equation (1) used by Milner-Brown et al. (1973) was slightly modified by Fuglevand et al. (1993), who initially modeled a muscle composed of 120 MUs. For $t = 0$ to t_{exp}:

$$F_{twFug}(t) = \frac{F_{\max}t}{T_c}\exp(1-\frac{t}{T_c}) \quad (3)$$

Here $F_{twFug}(t)$ is the force as a function of time caused by an impulse in T_{imp}. The following inequality constraint was also imposed: if $F_{twFug}(t) < F_{\max}/1000$, then $F_{twFug}(t) = 0$. Since the half-contraction time and the half-relation time could not be modified in Equation (3), the force curvature during the increasing and decreasing phases were uncontrolled. Note also that $T_{imp} = 0$ and T_{lead} were not included in Equation (3). However, the true time for each twitch with impulse in time T_{imp} was again *tau(t)* as in Equation (2).

Piotrkiewicz (1982) compared experimental twitches from animal muscles with the theoretical curve computed according to Equation (1), concluding that the experimental curves were very close to the theoretical curve when normalized to the two equation parameters. However, considerable differences were evident between the curves during approximation of the relaxation phases since the parameter T_{hr} was not accounted for and fixed (see Fig. 3 in Piotrkiewicz, 1982).

In 2002, we presented a 4-parameter twitch model (Raikova and Aladjov, 2002). Two new parameters, T_{hr} and T_{lead}, were included in the formulas:

$$F_{tw4par}(t) = p\left(t - T_{lead} - T_{imp}\right)^m \exp(-k(t - T_{lead} - T_{imp}))if\ t > T_{lead} + T_{imp}, \quad (4)$$

$$k = \frac{\ln 2}{T_{hr} - T_c - T_c\ln(\frac{T_{hr}}{T_c})} \quad (5)$$

$$m = kT_c \quad (6)$$

$$p = F_{\max}\exp(-kT_c(\ln T_c - 1)) \quad (7)$$

The following inequalities were also imposed: if $F_{tw4par}(t) < F_{\max}/1000$ then $F_{tw4par}(t) = 0$, and $T_{hr} > T_c$, $T_{tw} > T_{hr}$. $F_{tw4par}(t)$ was the twitch force in this model. Note that T_{lead} and T_{imp} are also included in Equation 4.

The 4-parameter model adequately described all experimentally recorded twitches (Raikova et al., 2007a; Raikova et al., 2007b). However, when decomposition of unfused tetanus into successive contractions was initiated (described in the next section), we found that the curvature of the twitch contraction phase was also important (hence T_{hc}), and its duration time should also be considered (hence T_{tw}; Raikova et al., 2008). We then developed a more complex 6-parameter analytical model:

$$F_{tw6par} = \frac{f_1(t)}{f_2(t)} \quad (8)$$

$$f_1(t) = F_{\max}(P1^{c1}\exp(c1 - c1P1) + (P2 - 1)P1^{c2}\exp(c2 - c2P1)) \quad (9)$$

$$f_2(t) = P2 + P2\exp(4\exp(1)P3) \quad (10)$$

$$P1(t) = (\frac{t - T_{imp} - T_{lead}}{T_c}) \quad (11)$$

$$P2(t) = 1 + \exp(2\exp(1)(P1 - 1)) \quad (12)$$

$$P3(t) = \frac{(t - T_{imp} - 0.5(T_{tw} + T_{hr}))}{T_{tw} - T_{Thr}} \quad (13)$$

$$c1 = \frac{\ln(2)T_c}{T_{hc} - T_c + T_c\ln(\frac{T_c}{T_{hc}})} \quad (14)$$

$$c2 = \frac{\ln(2)T_c}{T_{hr} - T_c + T_c\ln(\frac{T_c}{T_{hr}})} \quad (15)$$

Here $T_c > T_{hc}$.

Equations 8–15 actually described a 7-parameter model since T_{imp} was incorporated. However, time of the action potential is an input constant and does not influence the twitch curve and was included in Equations 8–15 for programming simplicity.

An experimentally recorded individual twitch and the four models

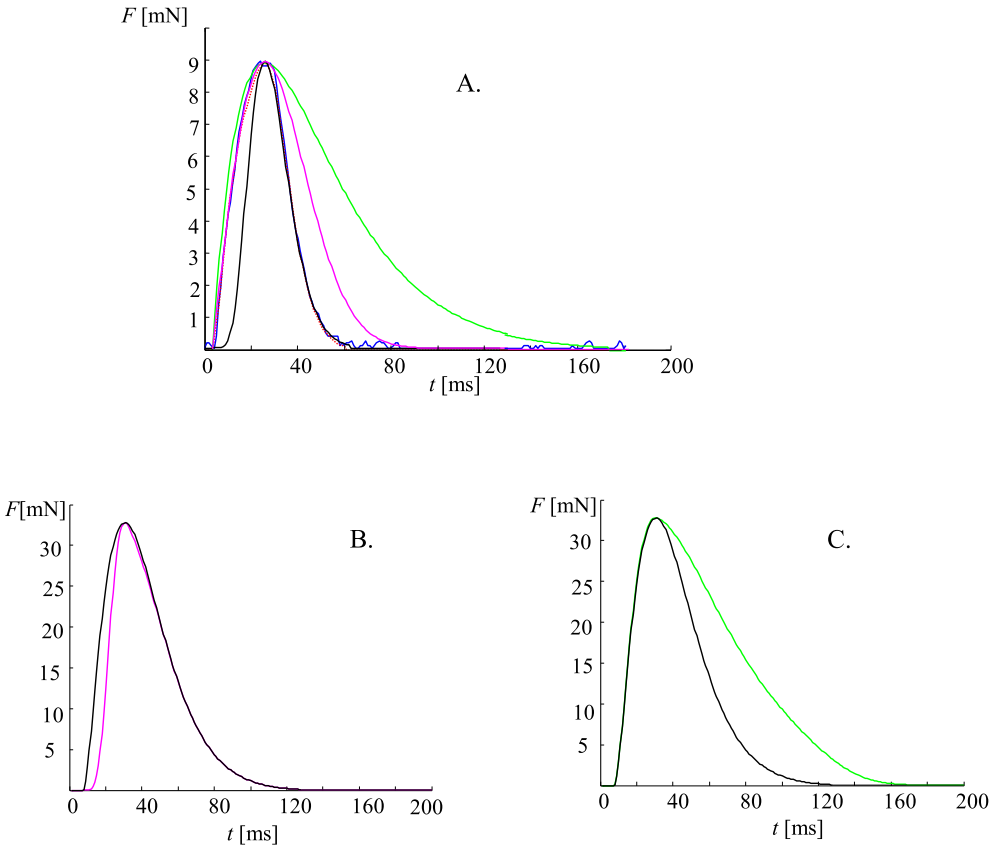

Fig. 2. A. Four twitch models compared to an experimental twitch contraction. Blue, the experimental recording of MU twitch force; green, Fuglevand's model; magenta, Piotrkiewicz's model; black, the 4-parameter model; red, the 6-parameter model (parameters: $T_{lead} = 3.4$, $T_{hc} = 7$, $T_c = 22.5$, $T_{hr} = 34$, $F_{max} = 8.9$, $T_{tw} = 100$, and $T_{imp} = 0$; mean squared errors between the experimental curve and the four models are as folows: 4.6995 for Fuglevand's model, 0.7339 for Piotrkiewicz's model, 0.08799 for 4-parameter model, 0.0159 for 6-parameter model). Note that the curve calculated using the 6-parameter model fits the experimental curve the nearly perfectly. B. The influence of the parameter T_{hc} on the twitch shape (the 6-parameters model is used). Black - $T_{lead} = 6.7$ ms; $T_c = 23.0$ ms; $T_{hc} = 8.1$ ms; $T_{hr} = 48.0$ ms; $F_{max} = 32.8$ mN; $T_{tw} = 200$ ms; $T_{imp} = 0$; magenta - $T_{lead} = 6.7$ ms; $T_c = 23.0$ ms; $T_{hc} = 14.0$ ms; $T_{hr} = 48.0$ ms; $F_{max} = 32.8$ mN; $T_{tw} = 200$ ms; $T_{imp} = 0$; C. The influence of the parameter T_{hr} on the twitch shape (the 6-parameters model is used). Black - $T_{lead} = 6.7$ ms; $T_c = 23.0$ ms; $T_{hc} = 8.1$ ms; $T_{hr} = 48.0$ ms; $F_{max} = 32.8$ mN; $T_{tw} = 200$ ms; $T_{imp} = 0$; green: $T_{lead} = 6.7$ ms; $T_c = 23.0$ ms; $T_{hc} = 8.1$ ms; $T_{hr} = 70.0$ ms; $F_{max} = 32.8$ mN; $T_{tw} = 200$ ms; $T_{imp} = 0$. (For interpretation of the references to colour in this figure legend, the reader is referred to the web version of this article.)

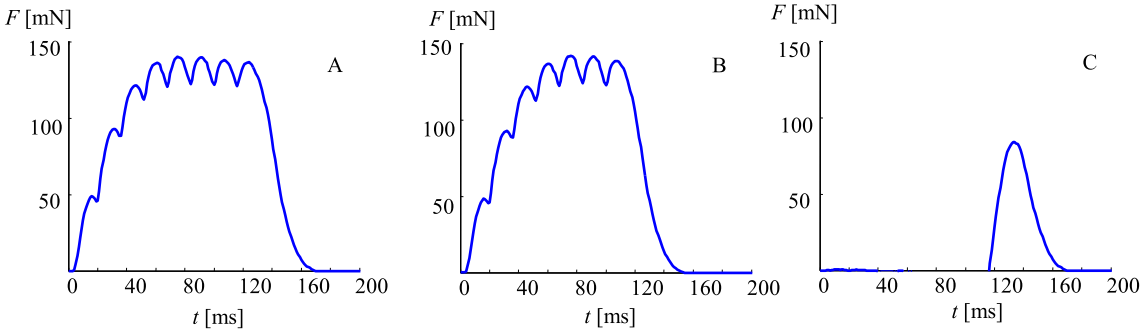

Fig. 3. Physiological confirmation of the twitch form shape of a response to one of stimuli used to induce the unfused tetanic contraction. Recordings for an FR type MU obtained from *in vivo* experiments based on electrical stimulation of single axons of motoneurons innervating the medial gastrocnemius in rat. **A.** A tetanus induced by eight action potentials delivered at a constant frequency. **B.** A tetanus induced by seven action potentials at the same constant frequency. The contraction caused by the eighth action potential was obtained by subtracting the experimental force curve in B from the one in A.

based on the above equations are shown in Fig. 2A. The Piotrkiewicz (1982) (Equation (1) and Fuglevand et al. (1993) (Equation (3) models could not fit the relaxation phase of the twitch. The curvature of the rising phase of the twitch also did not fit the experimental contractions using those two models. Note that the relaxation phase in the Fuglevand et al. (1993) (Equation (3) model is considerably longer since half-contraction time is not taken into account, contrary to the 6-parameter model (compare with Fig. 2b in Raikova et al., (2008) to see the influence of the last two parameters, T_{tw} and T_{hc}, in this model). It should be stressed that for unfused tetanic contractions, the course of relaxation is a crucial factor affecting force development because responses to successive action potentials usually begin at the relaxation phase of the preceding response. Fig. 2B and 2C illustrates a role of the T_{hc} and T_{hr}, which enables us to considerably change the twitch shape even when remaining 4 parameters remain constant. The decomposition of tetanic contractions into twitch responses to individual activations revealed that twitch shapes vary considerably (Raikova et al., 2007b) and simulation of these variable shapes requires flexible model of the twitch. It should be stressed that simplified models (in this case, those proposed by Piotrkiewicz (1982) and by Fuglevand et al. (1993), despite their usefulness in many simulation studies mentioned earlier, are unable to sufficiently and precisely describe changes in twitch shapes, especially during summation of individual twitches into tetanic contractions (Celichowski et al., 2014).

It has to be noted that other modifications of Fuglevand equation (3) exist. For example in Roatta et al. (2008) the function of the twitch force is devided into two parts – one for the contraction phase (before T_c) and one for the relaxation phase (after T_c). This is based on an asumption that the half-relaxation time is aproximate 5/3 from T_c. Similar approach is used in Negro and Orizio (2017). Our 6-parameters model

(equations 8–15) describe twitch force as one function where the only restriction for T_{hr} is to be bigger that T_c.

The modeled twitches can be incorporated into a whole muscle model (Fuglevand et al., 1993; Raikova et al., 2018), and this helps to avoid noise observed in experimental data (Fig. 2, blue line). In the study of Raikova et al. (2007b), 115 MUs were examined and modeled: 17 S, 58 FR, and 40 FF. The modeling process was semi-automatic, and the 4-parameter model (Equation 4) was used. The parameters F_{max}, T_c, and T_{hr} were estimated automatically, and T_{lead} was visually obtained. Then, F_{max}, T_c, and T_{hr} were visually corrected to match the experimental and modeling curves as closely as possible. The 4-parameter model approximated all individual twitches of different MU types with high precision, the most difficult being lead-time estimation. All twitches appeared different, and their force and time parameters were not duplicated. They were distributed continuously in an exponential manner (see Fig. 4 in Raikova et al., 2007b) with overlapping ranges for different MU types (see Table 1 in Raikova et al., 2007b). S MUs could be distinguished from FR and FF MUs based on their longer contraction and half-relaxation times and lower contraction velocity. However, such a distinction could not be made between FR and FF MUs.

4. Decomposition of the MU tetanic contraction

The twitches are relatively short. In rat medial gastrocnemius, their contraction times are 10–26 ms (Krutki et al., 2006), while those of their respective human muscles are 40–110 ms (Garnett et al., 1979). When muscles work, their motoneurons generate trains of action potentials at intervals shorter than the duration of twitches, so the muscle fibers respond to subsequent potentials with trains of overlapping twitch-shape forces, which are summed into tetanic contractions. The firing rate of motoneurons is limited by peripheral and descending inhibitory inputs and recurrent inhibition from Renshaw cells. Moreover, during voluntary contractions motoneurons exhibit firing rate saturation, which is likely caused by intrinsic mechanisms that prevent further increases in firing rate in the presence of increasing synaptic excitationis and is related to several intrinsic mechanisms (Fuglevand et al., 2015). The firing rates are also shaped by afterhyperpolarization following each action potential of the motoneuron, so the mean discharge rate during voluntary contractions is usually matched to the contractile properties of muscle fibers (Gardiner and Kernell, 1990; Bakels and Kernell, 1993). Consequently, twitch-shape responses to successive action potentials overlap, and MUs generate unfused tetanic contractions. Such force oscillations of each MU are the basic mechanism of the physiological tremor, which is observed in all voluntary movements (Halliday et al., 1999). At higher firing rates, force oscillations fade out, and the contraction develops fused tetanus of the highest possible force. A degree of fusion of a tetanic contraction is described by a fusion index, which varies from 0 for subtetanic twitches to 1 for fused tetanic contractions (Celichowski and Grottel, 1995).

In modeling the muscle or MU activity, the summation of twitch responses to successive contraction most frequently was assumed to be a linear process in which all responses to repeated stimuli have constant amplitude and duration (Raikova et al., 2013). As shown in Raikova et al. (2013), if interpulse intervals (IPIs) are equal and all MUs are synchronously activated, a constant mean level of the muscle force is achieved. This linearity implies that the neuronal signal is the determining factor of MU force, and the current physiological MU status can be omitted. From a mathematical perspective, the summation of equal twitches is the simplest approach. However, electrophysiological experiments on isolated MUs showed that the summation processes of twitch responses into tetanic force are nonlinear. First observations of such non-linearities were reported by Burke et al. (1976), who observed considerable changes in the MU forces in cat muscles, which were dependent on activation history and different in intensity and duration for different MU types. Later, Stein and Pagmiggiani (1979) recorded tetanic contractions of cat slow (soleus) and fast (plantaris) muscles, then subtracted the force produced by the j-1 stimulus from the one produced by the j^{th} stimulus. This approach calculated the contribution of the j^{th} stimulus to the total force and compared the result with the response to one stimulus (the twitch). They concluded that twitch-shape responses to individual stimuli summed into tetanus were stronger and had a longer duration than the separately recorded twitch.

Piotrkiewicz et al. (1986) observed considerable non-linearity in tetanic force development processes, finding that the weakest, predominantly S MUs, had the greatest ability to increase their force during tetanic contractions over the force predicted by algebraic summation of individually recorded twitches (Piotrkiewicz and Celichowski, 2007). Therefore, the simplified approach assuming that tetanic contractions are effects of summation of equal twitches appeared inadequate to describe complex processes of contractile force development, especially of S MUs. Observations based on the concept proposed by Stein and Parmiggiani (1979) (as illustrated in Fig. 3) were later tested on fast and slow MUs of the rat gastrocnemius muscle, for which progressive changes in twitch responses to 16 stimuli at constant IPIs were calculated (Raikova et al., 2008). Simulation of response shapes received in these experiments showed that the 6-parameter twitch model could precisely match the various twitch shapes obtained. S MUs showed greater variability in twitch response parameters than FR and FF MUs. The least variable parameter was lead time.

Experiments based on the method of Stein and Parmiggiani (1979) on functionally isolated MUs were performed on anesthetized rats using electrical stimulation of single axons of motoneurons innervating the medial gastrocnemius (for surgery and technical details see Drzymała-Celichowska and Celichowski, 2020). These studies revealed that for a set of MU force recordings obtained in response to progressively increasing stimuli numbers encountered a problem with fast MUs, which showed considerable potentiation and fatigue during repeated contractions, resulting in unstable twitch force levels. Therefore, we developed an innovative method for unfused tetanus decomposition, seeking to analyze force development processes in greater detail during unfused tetanic contractions recorded in electrophysiological experiments, which was initially applied for tetanic contractions induced at constant IPIs (Raikova et al., 2007a). While the term “decomposition” in biomechanics and physiology is often associated with surface

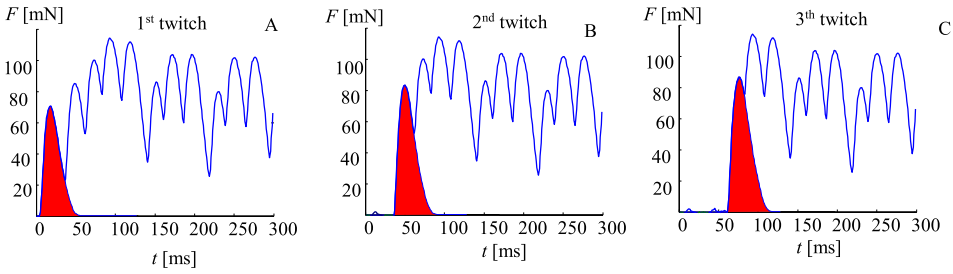

Fig. 4. Explanation of the decomposition method of a MU contraction into twitch-shape responses. **A.** Determination of the parameters of the first twitch ($T_{lead}1 = 4.3$, $T_c1 = 13.5$, $T_{hc}1 = 4.6$, $T_{hr}1 = 27.5$, $F_{max}1 = 70.5$, $T_{tw}1 = 65$, and $T_i1 = 0$). **B.** The tetanic force curve after subtracting the first twitch to determine the parameters of the second twitch ($T_{lead}2 = 4.5$, $T_c2 = 13.5$, $T_{hc}2 = 4.1$, $T_{hr}2 = 28.0$, $F_{max}2 = 83.3$, $T_{tw}2 = 69$, and $T_i2 = 32$). **C.** The tetanic force curve after subtracting the first and second twitches to determine the parameters of the third twitch ($T_{lead}3 = 4.5$, $T_c3 = 14.5$, $T_{hc}3 = 4.4$, $T_{hr}3 = 30.5$, $F_{max}3 = 87.0$, $T_{tw}3 = 70$, and $T_i3 = 57$).

electromyography (EMG) signal decomposition (De Luca et al., 2006) into trains of MU action potentials, the decomposition of the tetanus force was based on a completely different procedure.

The main concept of this method was presented by Celichowski et al. (2014) and is illustrated in Fig. 4. These experiments were performed on MUs of the rat medial gastrocnemius. Initially, a single separately recorded twitch was modeled with the 6-parameter model to determine the input values of the six parameters for this first contraction. Then, this twitch model was slightly modified to match the visible part of the first contraction within the tetanic recording (Fig. 4A), and the first twitch model was subtracted from the experimental curve. Consequently, the remaining part of the recorded force was exposed (Fig. 4B). This procedure was repeated for the second twitch (visible as the first one), for which twitch parameters were matched. For the third twitch, the sum of the first two twitch models was subtracted from the experimental curve (Fig. 4C), exposing the third contraction, and its model parameters were calculated. For each contraction, summing up into unfused tetanus, the parameters T_{hr} and T_{tw} could usually not be calculated automatically. The rules during additional manual estimation included moderate modification of the parameters of the twitch-shape response to preceding stimulus, well-describing the visible part of relaxation, and resembling the shape of the preceding twitch. An identical procedure was repeated until the last contraction. Consequently, a train of twitch-shape responses to individual action potentials was obtained for a MU, and the changes in twitch parameters were subject to the analysis (Fig. 5). A limitation of this method is that at least part of the relaxation phase must be visible to enable adjustment of parameters describing the relaxation (i.e., T_{hr} and T_{tw}). Therefore, decomposition is possible for tetani with a fusion index < 0.7, and the more fused a tetanus is, the less precise the decomposition process. Decomposition based on this method is impossible for fused tetanus.

Significant variability in twitch parameters for successive responses to individual stimuli was first noted for tetanic contractions at constant stimulation frequency. This observation turned our attention to the analysis of force development processes in tetanic contractions induced by trains of stimuli at variable IPIs. This approach appeared more suitable because, during voluntary motor activity, motoneurons generate action potentials at variable intervals (Moritz et al., 2005, Westergaard and De Luca, 2001). Therefore, this decomposition method was applied to tetani recorded for stimulation patterns with unequal IPIs, but at a given mean frequency, individually matched for different MUs to induce the unfused tetanic responses (Fig. 6; Celichowski et al., 2014). This study found considerable differences in the variability of decomposed twitch parameters between the three MU types (S, FR, and FF). The most surprising finding was the much higher amplitudes and larger twitch areas of the strongest decomposed twitch responses compared to separately recorded single twitches (up to 16-fold) observed for S MUs. However, some decomposed FF MU twitch responses had lower amplitudes than single twitches. The precision of the decomposition was later assessed by comparing the force curve recorded and modeled by summing the decomposed twitch models, finding a fit coefficient $> 98\%$, confirming the high accuracy of this method (Raikova et al., 2016a).

5. Simulation of the MU tetanus force

It was clear from the modeling of decomposed twitches that the successive twitch contractions summing into unfused tetanus had different force and time parameters, which depended on the initial force level of the contraction. It should also be noted that for the three different MU types, the decomposed twitches had different relationships with the first twitch. In the commonly cited muscle model proposed by Fuglevand et al. (1993), three MU types were not distinguished, but the amplitudes of simulated MU twitches were variable and assigned according to the rank in the recruitment order (the size principle), whereas twitch contraction times were inversely related to the twitch amplitude as was observed in numerous experimental studies. A gain was used to change the amplitude of successive contractions, and this parameter depended on IPIs. Namely, to calculate the tetanic forces of MUs

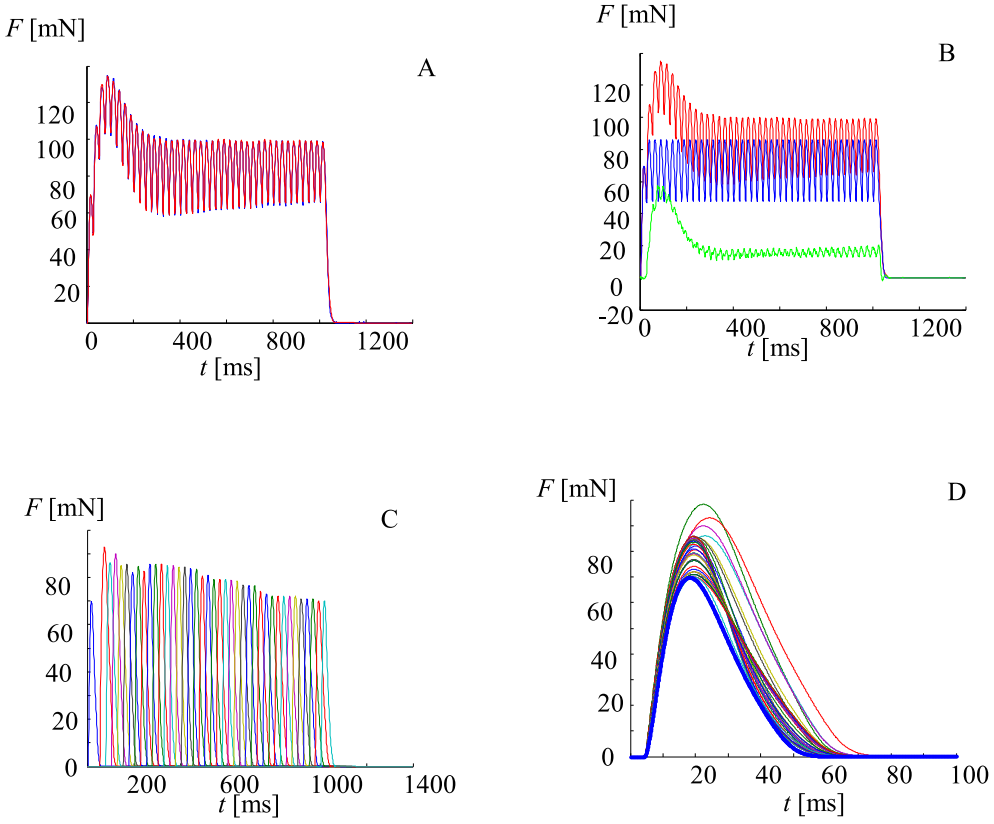

Fig. 5. An example of tetanic curve decomposition for an FR type MU of the rat medial gastrocnemius stimulated at a constant frequency of 40 Hz. **A.** The recorded force (red trace) and the force reconstructed as the sum of all decomposed twitches (blue trace). **B.** The recorded force (red trace) and the force reconstructed as the sum of twitches of constant parameters (equal to a single twitch, blue trace), and the difference between the two recordings (green trace), illustrating that the force recorded is higher than values predicted by simple modeling. **C.** The successive decomposed twitches are presented on a time scale according to their appearance. **D.** The twitches decomposed from the tetanic recording, presented on an enlarged time scale, and overlapped, assuming that T_{imp} for all applied stimuli is 0. Note differences in amplitude and duration between individual decomposed twitch responses. (For interpretation of the references to colour in this figure legend, the reader is referred to the web version of this article.)

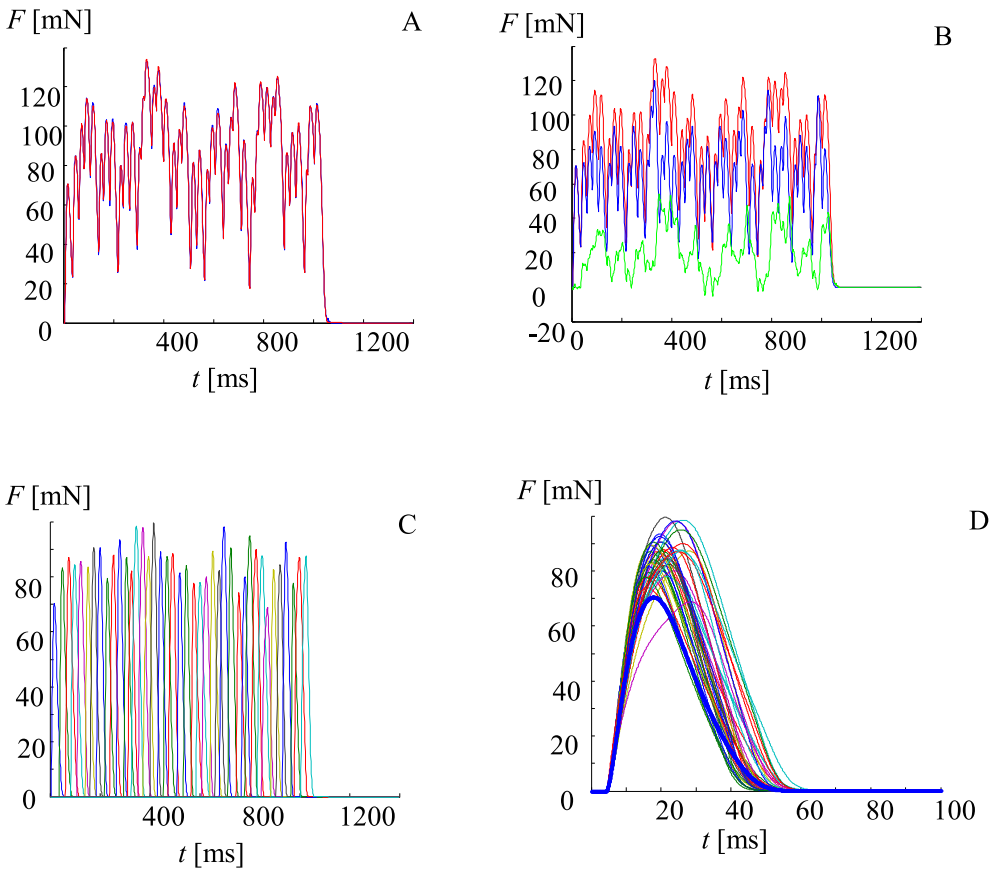

Fig. 6. An example of tetanic curve decomposition for an FR type MU of the rat medial gastrocnemius (the same as in Fig. 5) stimulated at a mean frequency of 40 Hz but with variable IPIs. **A.** The recorded force (red trace) and force reconstructed as the sum of all decomposed twitches presented (blue trace). **B.** The recorded force (red trace) and the force reconstructed as the sum of twitches with constant parameters (equal to the single twitch, blue trace) and the difference between the two above recordings (green trace), illustrating that the force recorded is higher than values predicted by the simple modeling. **C.** The successive decomposed twitches are presented on a time scale according to their appearance. **D.** The twitches decomposed from the tetanic recording, presented on an enlarged time scale, and overlapped, assuming that T_{imp} for all applied stimuli is 0. Note differences in amplitude and duration between individual decomposed twitch responses. (For interpretation of the references to colour in this figure legend, the reader is referred to the web version of this article.)

nonlinear force-firing rate behavior was simulated by varying MU force gain as a function of the instantaneous firing rate of motoneuron and the contraction time of the unit. Finally, the total muscle force was computed as the sum of individual MU forces.

To model the dynamic changes of parameters of twitches summing into tetanic contractions for studied by us MUs of rat gastrocnemius, we used 30 tetanic curves (10 of each MU type with similar fusion degrees) obtained in electrophysiological experiments in which different irregular patterns composed of 41 stimuli were used to activate motor axons (Raikova et al., 2016b). The unfused tetani were decomposed, and the decomposed contractions were modeled using the 6-parameter model. The following parameters were determined for each modeled twitch: $F^{(j)}_{max}(i)$, $T^{(j)}_{lead}(i)$, $T^{(j)}_{hc}(i)$, $T^{(j)}_{c}(i)$, $T^{(j)}_{hr}(i)$, and $T^{(j)}_{tw}(i)$ where $i = 1, 2,\ldots, 41$ and $j = 1, 2,\ldots, 30$. The index i denoted the number of successive contractions within tetanus. The index j was assigned to different MUs, $j = 1, 2, \ldots, 10$ for slow MUs, $j = 11, 12,\ldots, 20$ for FR MUs, and $j = 21, 22, \ldots, 30$ for FF MUs. In addition to these parameters, the force level at which each successive contraction starts, $F^{(j)}_{tetmin}(i)$, was also calculated from the experimental force recording. The last parameter, $F^{(j)}_{mftf}$, was defined as the maximum tetanic force that a MU could develop, determined for each MU from the recorded fused tetanus induced at 150 Hz. $F^{(j)}_{res}(i) = F^{(j)}_{mftf} - F^{(j)}_{tetmin}(i)$ was the force that the MU could still develop at its current state before reaching its maximum force of fused tetanus. The lead time had low variability, so for modeling purposes, it was decided that $T^{(j)}_{lead}(i) = T^{(j)}_{lead}(1)$. Therefore, lead time was constant and equal to the lead time of the first decomposed twitch.

Different dependencies among these parameters were assessed. A steady relationship was found between $F^{(j)}_{max}(i)$ and $F^{(j)}_{res}(i)$, normalized to the amplitude of the first decomposed twitch of the respective MU (i.e., $F^{(j)}_{max}(1)$) for all 30 MUs (see Fig. 3 in Raikova et al., 2016b). For each MU, a linear approximation of the points $(F^{(j)}_{res}(i)/F^{(j)}_{\max}(1), F^{(j)}_{\max}(i)/F^{(j)}_{\max}(1))$ was found and the angles $\alpha^{(j)}$ between the approximation lines and y-axis were calculated. This angle was specific for each MU. It was smallest

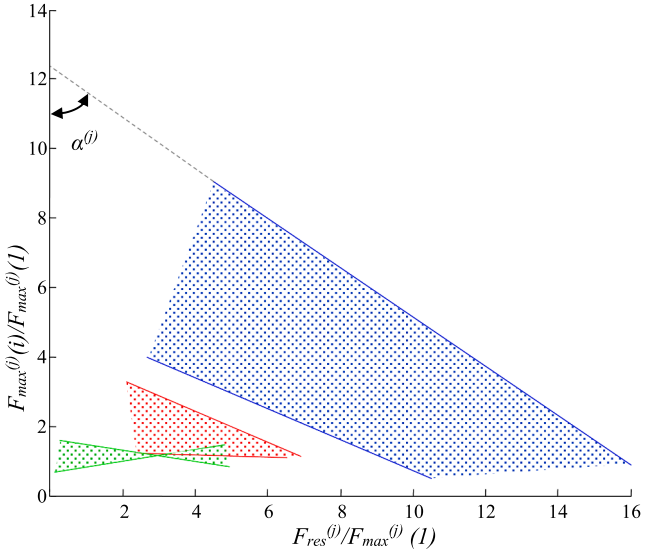

Fig. 7. Dependencies between two normalized parameters, $F_{max}(j)(i)/F_{max}(j)(1)$ and $F_{res}(j)(i)/F_{max}(j)(1)$, for the three MU types used in the model of the rat medial gastrocnemius muscle. The angle $\alpha^{(j)}$ calculated separately for each MU determines the force development processes for a given MU within the unfused tetanic contraction. Two border lines are presented for each MU type, while the lines obtained for all remaining MUs within each type cover areas described by different colors. Blue, S MUs; red, FR MUs; green, FF MUs. (For interpretation of the references to colour in this figure legend, the reader is referred to the web version of this article.)

for S MUs, higher for FR MUs, and highest (even > 90°) for FF MUs. Its values did not overlap for slow and fast MUs (Fig. 7). For all S and FR MUs, the linear approximation of the dependence between $F_{res}^{(j)}(i)/F_{\max}^{(j)}(1)$ and $F_{\max}^{(j)}(i)/F_{\max}^{(j)}(1)$ and calculated angles indicated that the amplitudes of subsequent contractions within tetanus increased when the developed force was closer to the maximal fused tetanic force. This increase was higher for S MUs with a smaller $\alpha^{(j)}$ angle. However, the amplitudes had a different limit for each MU type. This limit was not reached for S MUs, probably because the tetanic curves were moderately fused, and the capacity of S MUs to develop higher force was larger than that of FR and FF MUs. Smaller force amplitudes of S MU contractions were observed when the force level at which the contraction started was far from the maximal possible MU force. For some FF MUs with $\alpha^{(j)} > 90°$, the above dependencies were opposite: the contraction amplitudes increased with increasing residual force.

The relationship between $\alpha^{(j)}$ and the parameter $F_{mftf}^{(j)}/F_{\max}^{(j)}(1)$ was the most promising for modeling. Moreover, the two other parameters, $F_{mftf}^{(j)}$ and $F_{max}^{(j)}(1)$ (i.e., the maximum possible MU force and the amplitude of the single twitch, respectively), were easily definable and specific for each MU type. Several approximations of the above relationship with different linear and nonlinear functions were explored using MATLAB functions (see Fig. 4 in Raikova et al., 2016b). A power model was determined to be the most suitable for our purposes. Consequently, the angle $\alpha^{(j)}$ was calculated as:

$$\alpha^{(j)} = 108.8\left(F_{mftf}^{(j)}/F_{\max}^{(j)}(1)\right)^{(-0.2603)}$$

With the specific angle $\alpha^{(j)}$ for a given MU type and accounting for the linear regression of $F_{res}^{(j)}(i)/F_{\max}^{(j)}(1)$ on $F_{\max}^{(j)}(i)/F_{\max}^{(j)}(1)$, the amplitude of the i^{th} contraction within a tetanic curve could be calculated for the j^{th} MU as:

$$F_{\max}^{(j)}(i) = (1 + \cot(\alpha^{(j)})F_{tetmin}^{(j)}(i)/F_{\max}^{(j)}(1))F_{\max}^{(j)}(1) \quad (17)$$

The parameters of successive twitch-like responses, contraction and half-relaxation time, were hypothesized to depend on the actual MU force level at which the i^{th} contraction started (i.e., $F_{tetmin}^{(j)}(i)$) and were calculated as (see Fig. 5 in Raikova et al., 2016b):

$$T_c^{(j)}(i) = (1.04 + 0.274F_{tetmin}^{(j)}(i)/F_{\max}^{(j)}(1))T_c^{(j)}(1) \quad (18)$$

$$T_{hr}^{(j)}(i) = (2.397 + 0.3509F_{tetmin}^{(j)}(i)/F_{\max}^{(j)}(1))T_c^{(j)}(1) \quad (19)$$

The remaining two parameters, half-contraction time and twitch duration, were intended to be changed proportional to the contraction and half-relaxation times, respectively, and calculated as:

$$T_{hc}^{(j)}(i) = T_{hc}^{(j)}(1)(T_c^{(j)}(i)/T_c^{(j)}(1)) \quad (20)$$

$$T_{tw}^{(j)}(i) = T_{tw}^{(j)}(1)(T_{hr}^{(j)}(i)/T_{hr}^{(j)}(1)) \quad (21)$$

In this model, all 30 tetanic curves and three additional tetani were modeled (see Fig. 8 in Raikova et al., 2016b). Differences between experimental and modeled curves were evaluated using two coefficients (see Table 1 in Raikova et al., 2016b). It was concluded that this model predicted the tetani more precisely than the summation of equal twitches, especially for S MUs. Based on the sensitivity analysis and including the three new tetani, Equation 16 was adjusted to:

$$\alpha^{(j)} = 117.2\left(F_{mftf}^{(j)}/F_{\max}^{(j)}(1)\right)^{(-0.3144)} \quad (22)$$

The calculated angles $\alpha^{(j)}$ varied between 53.89° and 95.87°, increasing from S to FF MUs (Fig. 7). For three FF MUs, this angle exceeded 90^0. When this angle was equal to 90°, the successive twitch-shape contractions had the same maximal force, independent of the stimulation pattern, but might have different time parameters. For most FF MUs, some values of $F_{\max}^{(j)}(i)/F_{\max}^{(j)}(1)$ were < 1, indicating that these decomposed contractions had amplitudes lower than the first contraction. This situation never occurred for S or FR MUs. In general, the angle $\alpha^{(j)}$ indicated whether the amplitudes of successive contractions within unfused tetanus would increase ($\alpha^{(j)} < 90°$), remain constant ($\alpha^{(j)} = 90°$), or decrease ($\alpha^{(j)} > 90°$) during tetanic force development. The maximal calculated angle was 117.2°, and the minimal was 45.7° (Raikova et al., 2016b). In summary of the above, the angle α is a mathematical parameter proposed to calculate the expected MU force at different firing frequency ranges, even for variable stimulation patterns for MUs of three physiological types. It is rather impossible to indicate contractile properties directly related to this mathematical parameter. The angle α reflects predominantly differences between MUs in the force sensitivity to changes in the stimulation frequency, and a range of possible changes in force between the twitch (the minimum force) and the fused tetanus (the maximum force).

It should be noted that the experimental data concerned rat medial gastrocnemius muscle MUs and would be different for other muscles. Indeed, the decomposed tetani had similar fusion indices (obtained at different mean frequencies and firing patterns), so the areas in Fig. 7 would be different, changing the fusion index. The proposed approach for predicting successive contractions within unfused tetani reflected more realistic conditions than the methods in which summation of equal twitches was performed or only twitch amplitudes were changed depending on previous IPIs.

6. Models of muscle based on MU recruitment

The realism of a muscle model composed of a set of MUs has three major aspects: (1) the adequate number and proportion of different MU types within a muscle; (2) the adequate expression of the mechanical aspects, i.e., the force developed by individual MUs (twitch), summation of these twitches into tetanus, and summation of forces of recruited MUs into the whole muscle force; (3) the appropriate principles of the force control (i.e., the recruitment and decruitment of MUs and their firing rates and discharge patterns).

Several studies have proposed muscle models composed of MUs. Most adopted or extended Fuglevand's model (Fuglevand et al., 1993), consisting of 120 MUs in a pool, unconnected with any real muscle. Their primary objective was to investigate how this pool was organized to regulate muscle force (i.e., how MUs were recruited and their firing rates were changed) and compare simulated results with simulated surface EMG signals during isometric contractions. The twitch forces of MUs were described using only two parameters, the maximal amplitude and contraction time (Equation (3). The relationship between contraction times and maximal amplitudes was fixed with a minimum contraction time of 30 ms and a maximum contraction time of 90 ms. The force amplitude distribution among these 120 MUs was modeled by an exponential function, and the force varied over a 100-fold range from the first MU (the lowest-threshold MU) with the smallest force to the last, 120th MU (the highest-threshold MU). Consequently, half of the MU pool had twitch amplitudes < 10% of the largest amplitude (see Fig. 1 in Fuglevand et al., 1993). A gain dependent on a preceding IPI and contraction time were included in the twitch force formula so that the twitch could be modified during the tetanus development. One excitatory signal ($E(t)$) was used for the whole pool, which could vary from zero (no MU is active) to 100% (all MUs are active). Moreover, the recruitment threshold of excitation (RTE(t)) was defined as the minimum $E(t)$ required to start a discharge in a motoneuron, which is an exponential function of the MU number. Then, the firing rate of a motoneuron was expressed as a linear function of $E(t)$ and $RTE(t)$, accounting for the minimum firing rate for each MU. The duration of each discharge was calculated based on the firing rate, and random constants were added to the calculated IPIs to avoid synchronization between MUs. This model was used to simulate the muscle force at different values of $E(t)$ and firing frequencies and compared with simulated EMGs, identifying a nonlinear EMG-muscle force relationship.

The same model was used to investigate muscle fatigue (Potvin and

Fuglevand, 2017), modeled by decreasing amplitudes of MU forces and increasing contraction times. The authors mentioned in this study that *E (t)* decreases with fatigue, altering firing rates, but such changes were not modeled.

A similar model for isometric contractions was proposed by Contessa and De Luca (2013) for two muscles, the vastus lateralis (containing 600 MUs) and the first dorsal interosseous (containing 120 MUs). The common drive hypothesis was adopted, and the excitation signal ranged from 0 to 1. Firing rates were inversely proportional to the recruitment threshold, so the "onion skin" property (De Luca et al., 1982; De Luca and Erim, 1994) was adopted. The twitches were modeled using the 4-parameter model of Raikova and Aladjov (2002). The nonlinear summation of twitches was accounted for with a gain factor that changed firing rates. The amplitudes of twitches summating into tetanus were also changed using a linear increase of the contraction in the first 60 s or 40 s for the two respective muscles, followed by a linear decrease. This approach was associated with the logic of potentiation and fatigue. The study considered real muscles but did not distinguish between slow and fast MUs, and the twitches of all MUs were homogeneously distributed. The forces of all MUs were summed linearly to obtain the whole muscle force. Moreover, the study included force feedback in the model, changing certain parameters in a loop to reach the given simulated muscle force. They observed an increase in the force oscillations during long contractions caused by the progressive recruitment of larger fast MUs.

Petersen and Rostalski (2019) also used a modified Fuglevand's model to investigate the EMG-force relationship in isometric conditions through simulations of the rectus abdominis muscle comprising 300 MUs. They proposed a feed-forward model in which the excitation signal was calculated in the range of 0 to 1 based on the muscle force. The main objective was to scale almost all model parameters according to the size principle, and the recruitment order was slightly modified compared to Fuglevand et al. (1993). The twitch forces were calculated using the 4-parameter model of Raikova and Aladjov (2002) with peak twitch forces modeled as a linear function of recruitment thresholds. The time parameters were sampled using the Weibull distribution. Twitch amplitude was a linear function of the recruitment threshold and decreased at higher firing rates. The summation of successive twitches into tetanus was linear.

Recently, Huang et al. (2021) used Fuglevand's model with 120 MUs to study the consequences of losing a certain number of MUs. They concluded that losing large MUs had a more significant effect on decreasing muscle strength than losing smaller MUs.

Compared to the studies described above, the muscle model presented by Raikova et al. (2018) included several elements that made it more realistic. It considered data from *in vivo* experiments on the rat medial gastrocnemius muscle, composed of 57 MUs, divided into three physiological types in the actual proportions observed for this muscle: 8 S, 23 FR, and 26 FF. They were selected from a pool of 300 MUs based on their twitch forces matching the means and ranges previously documented for particular MU types and the whole muscle. The measured twitches were precisely modeled using the 6-parameter model. Therefore, the twitch parameters were not modeled using linear or exponential functions and the ranges of force amplitudes and time parameters between MU types partly overlapped (see Table 1 and Fig. 1 in Raikova et al., 2018). The summation of twitches into tetanic contractions was nonlinear due to the random IPI patterns. Five parameters (lead time was equal for each successive twitch) were calculated according to the regression equations obtained based on the decomposition of unfused tetani experimentally recorded for different stimulation patterns (Raikova et al., 2016b). The calculations used a specific angle calculated for each MU from the relationship between the maximum fused tetanic force and the amplitude of the individual single twitch. The recruitment threshold of motoneurons and the respective equation for its calculation were based on experimentally recorded values of the rheobase current, and the common drive hypothesis was adopted. The mean, minimum, and maximum discharge frequencies were individually calculated based on the steady-state rhythmic firing frequencies measured in electrophysiological experiments on a large population of rat medial gastrocnemius motoneurons. In fact a complex interplay between excitatory and inhibitory inputs from descending tracts and the periphery produces the discharges of motoneurons (Macefield et al., 1993; Binder et al., 2002). Alhough a net excitatory effect is necessary to maintain a depolarization of motoneuron's membrane potential, inhibitory inputs are also essential regulators of motoneuron excitability, but for modeling purposes the situation was simplified and only excitatory signal was taken as a unique input to simulated pool of motoneurons. The excitation signal ranged from 0 to 100. The model investigated two types of excitation signals, a triangular one and a trapezoid one, with a steady-state phase for 2 s. The relative participation of all three MU types was examined to determine their different roles during contractions at different excitation levels. It was concluded that even for eight relatively weak S MUs in the model, their role in generating the whole muscle force was remarkable due to the effective summation of their twitches into tetanus. Moreover, S MUs appeared to play a specific role in smoothing the movements due to low force oscillations observed during the summation of all S MU forces.

The major disadvantage of this model was its specificity for a particular rat muscle since the twitch parameters, regression equations, and respective motoneuron properties would be considerably different for other muscles. However, it would be possible to adapt the same principles and recalculate the parameters in models of other muscles.

7. Application of MU and muscle models

The modeling of muscle force based on the assumption that it represents the summation of forces generated by individual MUs recruited into a muscle contraction is a convenient tool for studying processes determining the motor output, relevant to several motor control processes in the central nervous system. Some of these processes can be simulated by shaping the firing patterns of individual motoneurons. Electrophysiological studies on the significance of active MU firing rate have examined numerous human muscles during their voluntary contractions (Zero et al., 2022; Bailey et al., 2007; Cabral et al., 2018). They found various levels of motoneuron discharge synchronization, but the functional role of synchronization was not completely clear (Farina and Negro, 2015). Fuglevand's model (Fuglevand et al., 1993) was also used to study the effects of MU synchronization (Yao et al., 2000; Santello and Fuglevand, 2004). The same problem was recently explored by Raikova et al. (2021) with the additional objective of evaluating the role of particular MU types in physiological tremor, which is related to synchronization level.

In recent decades, the dynamic progress in motor control research has come from studies of motoneuronal firing patterns during voluntary contractions based on EMG decomposition (Enoka, 2019). This impressive technique delivered appreciable data illustrating activities and strategies of motoneurons in various muscles and during variable motor tasks. However, as indicated above, MU force production is a nonlinear process, and individual MU action potentials visible in a decomposed EMG may have an unequal influence on MU force, despite being constant in shape and amplitude (Celichowski et al., 2014). Therefore, MU force decomposition is a valuable tool that might help to increase our understanding of the functional role of motoneuronal rate coding in force output control. The described decomposition technique was used to explain the sag mechanism in unfused tetanic contractions of fast MUs (Kryściak et al., 2019). The transitory force decrease phenomenon related to high-frequency stimulation preceding the lower frequency tetanus phase was also evaluated with this method (Rakoczy et al., 2020), and sex differences in the rate coding and force development of rat soleus MUs were investigated (Drzymała-Celichowska et al., 2015). This method was recently used to decompose single MU signals during the tetanic activities of human biceps brachii during voluntary

slow isometric contractions studied using an ultrafast ultrasound method (Rohlén et al., 2022). Twitch-shape response parameters of the studied MUs were dependent on preceding IPIs, indicating a considerable similarity to data obtained by animal studies, demonstrating that certain force development processes in muscles of different mammals can be similarly modeled.

The muscle models proposed to date have certain limitations, as several physiological properties observed in active MUs and muscles have not been incorporated. This concerns, for example, potentiation and fatigue occurring in fast MUs (Kernell et al., 1975). These processes develop within a few tens of seconds, so their absence influences the realism of prolonged contraction models. Another limitation concerns some nonlinear force production processes documented mainly for fast MUs as sensitivity to changes even in a single IPI, including a catch-like effect (Burke et al., 1976), tetanic depression (Celichowski et al., 2011), the boost in force at the beginning of activity (Kryściak et al., 2020), which have not been predicted in modeling to date. Finally, the proposed models assume that muscle output force is a cumulative sum of individual MU forces, while this process is more complex. Coactivation of two or more MUs within a muscle often leads to contradictory results, as a cumulative force can be higher or lower than a sum of MUs forces. Apart from differences between individual muscles, this depends mostly on MU type, the number of co-active MUs, muscle architecture, and their location within a muscle (Emonet-Dénand et al., 1987; Clamann and Schelhorn, 1988; Sandercock, 2000; Sandercock, 2003; Drzymała-Celichowska et al., 2010). The discrepancies in contractile properties of different MUs undoubtedly influence the results of muscle force modeling. Moreover, all muscles have individual unique properties; they differ in architecture, size, MUs composition, and function. Therefore, in order to increase the realism of the simulated muscle force, as many as possible input data for the model should be individually matched for each muscle.

The present review concerned several approaches in modeling of MU and muscle force, proposed by different laboratories. We believe that significant challenges in this field are nonlinearity of force production processes as well as interspecies differences and variability of MU contractile properies between individual muscles. A major difficulty in human muscle modeling is related to limited data on contractile properies of their MUs. From this reason a direct adaptation of the rat model of a twitch and summation of twitches into tetanic contractions based on the angle α to human muscles would also be hardly possible. On the other hand, one may expect progress with new methods of human MUs' twitch imaging. The recently proposed minimally invasive micro-endoscopy (Sanchez et al., 2015) revealed that sarcomere displacement and twitch force exhibited nearly identical dynamics. Another non-invasive technique of ultrafast ultrasound imaging (Rohlén et al., 2022) illustrated human MU twitches and unfused tetanic contractions profiles, and validated the 4-parameter twitch model proposed originally for rat MUs (Raikova and Aladjov, 2002). These new directions can provide a more precise quantitative representation of the muscle, which is a key to new approaches in modeling of human muscle.

Declaration of Competing Interest

The authors declare that they have no known competing financial interests or personal relationships that could have appeared to influence the work reported in this paper.

Acknowledgements

The study was supported by Joint Polish-Bulgarian Research Project for years 2022-2023.

References

Bailey, E.F., Rice, A.D., Fuglevand, A.J., 2007. Firing patterns of human genioglossus motor units during voluntary tongue movement. J. Neurophysiol. 97 (1), 933–936.
Bakels, R., Kernell, D., 1993. Matching between motoneurone and muscle unit properties in rat medial gastrocnemius. J. Physiol. 463, 307–324.
Bigland-Ritchie, B., Fuglevand, A.J., Thomas, C.K., 1998. Contractile properties of human motor units: Is man a gat? Neuroscientist 4 (4), 240–249.
Binder, M.D., Heckman, C.J., Powers, R.K., 2002. Relative strengths and distributions of different sources of synaptic input to the motoneurone pool: implications for motor unit recruitment. Adv. Exp. Med. Biol. 508, 207–212. https://doi.org/10.1007/978-1-4615-0713-0_25.
Brown, I.E., Cheng, E.J., Loeb, G.E., 1999. Measured and modelled properties of mammalian skeletal muscle. II. The effects of stimulus frequency on force-length and force-velocity relationships. J. Muscle Res Cell Motility. 20 (7), 627–643.
Burke, R.E., 1981. Motor units: anatomy, physiology and functional organization. In: Brooks, V.B. (Ed.), Handbook of Physiology Section 1: The Nervous System, Vol. 1, Part 1. American Physiological Society, Bethesda, MD, pp. 345–422.
Burke, R.E., Levine, D.N., Tsairis, P., Zajac, F.E., 1973. Physiological types and histochemical profiles in motor units of the cat gastrocnemius. J. Physiol. 234 (3), 723–748.
Burke, R.E., Rudomin, P., Zajac, F.E., 1976. The effect of activation history on tension production by individual muscle units. Brain Res. 109 (3), 515–529.
Cabral, H.V., de Souza, L.M.L., Mello, R.G.T., Gallina, A., de Oliveira, L.F., Vieira, T.M., 2018. Is the firing rate of motor units in different vastus medialis regions modulated similarly during isometric contractions? Muscle Nerve 57 (2), 279–286.
Celichowski, J., Dobrzyńska, Z., Łochyński, D., Krutki, P., 2011. The tetanic depression in fast motor units of mammalian skeletal muscle can be evoked by lengthening of one initial interpulse interval. Exp. Brain Res. 214 (1), 19–26.
Celichowski, J., Grottel, K., 1995. The relationship between fusion index and stimulation frequency in tetani of motor units in rat medial gastrocnemius. Arch. Ital. Biol. 133 (2), 81–87.
Celichowski, J., Raikova, R., Aladjov, H., Krutki, P., 2014. Dynamic changes of twitch-like responses to successive stimuli studied by decomposition of motor unit tetanic contractions in rat medial gastrocnemius. J. Neurophysiol. 112 (12), 3116–3124.
Clamann, H.P., Schelhorn, T.B., 1988. Nonlinear force addition of newly recruited motor units in the cat hindlimb. Muscle Nerve 11 (10), 1079–1089.
Contessa, P., De Luca, C.J., 2013. Neural control of muscle force: indications from a simulation model. J. Neurophysiol. 109 (6), 1548–1570.
De Luca, C.J., Adam, A., Wotiz, R., Gilmore, L.D., Nawab, S.H., 2006. Decomposition of surface EMG signals. J. Neurophysiol. 96 (3), 1646–1657.
De Luca, C.J., Erim, Z., 1994. Common drive of motor units in regulation of muscle force. Trends Neurosci. 17 (7), 299–305.
De Luca, C.J., LeFever, R.S., McCue, M.P., Xenakis, A.P., 1982. Control scheme governing concurrently active human motor units during voluntary contractions. J. Physiol. 329, 129–142.
Dideriksen, J.L., Negro, F., 2018. Spike-triggered averaging provides inaccurate estimates of motor unit twitch properties under optimal conditions. J. Electromyogr. Kinesiol. 43, 104–110.
Drzymała-Celichowska, H., Celichowski, J., 2020. Functional isolation of single motor units of rat medial gastrocnemius muscle. J. Vis. Exp. 166 https://doi.org/10.3791/61614. PMID: 33427242.
Drzymała-Celichowska, H., Krutki, P., Celichowski, J., 2010. Summation of motor unit forces in rat medial gastrocnemius muscle. J. Electromyogr. Kinesiol. 20 (4), 599–607.
Drzymała-Celichowska, H., Karolczak, J., Rędowicz, M.J., Bukowska, D., 2012. The content of myosin heavy chains in hindlimb muscles of female and male rats. J. Physiol. Pharmacol. 63 (2), 187–193.
Drzymała-Celichowska, H., Raikova, R., Krutki, P., 2015. Decomposition of motor unit tetanic contractions of rat soleus muscle: Differences between males and females. J. Biomech. 48 (12), 3097–3102.
Elias, L.A., Chaud, V.M., Kohn, A.F., 2012. Models of passive and active dendrite motoneuron pools and their differences in muscle force control. J. Comput. Neurosci. 33 (3), 515–531. https://doi.org/10.1007/s10827-012-0398-4.
Elias, L.A., Kohn, A.F., 2013. Individual and collective properties of computationally efficient motoneuron models of types S and F with active dendrites. Neurocomputing 99, 521–533. https://doi.org/10.1016/j.neucom.2012.06.038.
Elias, L.A., Watanabe, R.N., Kohn, A.F., 2014. Spinal mechanisms may provide a combination of intermittent and continuous control of human posture: predictions from a biologically based neuromusculoskeletal model. PLoS Comput. Biol. 10 (11), e1003944.
Emonet-Dénand, F., Filippi, G.M., Laporte, Y., Petit, J., 1987. Sommation de tensions tétaniques maximales développées par des unités motrices lentes ou rapides du muscle long péronier du chat [Summation of maximal tetanic tensions developed by slow or fast motor units of the peroneus longus muscle in the cat]. C. R. Acad. Sci. III 305 (10), 417–422.
Enoka, R.M., 2019. Physiological validation of the decomposition of surface EMG signals. J. Electromyogr. Kinesiol. 46, 70–83. https://doi.org/10.1016/j.jelekin.2019.03.010.
Farina, D., Negro, F., 2015. Common synaptic input to motor neurons, motor unit synchronization, and force control. Exerc. Sport Sci. Rev. 43 (1), 23–33.
Fuglevand, A.J., Winter, D.A., Patla, A.E., 1993. Models of recruitment and rate coding organization in motor-unit pools. J. Neurophysiol. 70 (6), 2470–2488.
Fuglevand, A.J., Lester, R.A., Johns, R.K., 2015. Distinguishing intrinsic from extrinsic factors underlying firing rate saturation in human motor units. J. Neurophysiol. 113 (5), 1310–1322.

Gardiner, P.F., Kernell, D., 1990. The, "fastness" of rat motoneurones: time-course of afterhyperpolarization in relation to axonal conduction velocity and muscle unit contractile speed. Pflugers Arch. 415 (6), 762–766.
Garnett, R.A., O'Donovan, M.J., Stephens, J.A., Taylor, A., 1979. Motor unit organization of human medial gastrocnemius. J. Physiol. 287, 33–43.
Halliday, D.M., Conway, B.A., Farmer, S.F., Rosenberg, J.R., 1999. Load-independent contributions from motor-unit synchronization to human physiological tremor. J. Neurophysiol. 82 (2), 664–675.
Heckman, C.J., Enoka, R.M., 2012. Motor unit. Compr. Physiol. 2 (4), 2629–2682.
Henneman, E., 1957. Relation between size of neurons and their susceptibility to discharge. Science 126 (3287), 1345–1347.
Hennig R, Lømo T. Firing patterns of motor units in normal rats. Nature. 1985;14-20;314 (6007):164-6.
Huang C, Chen M, Zhang Y, Li S, Zhou P. Model-based analysis of muscle strength and EMG-force relation with respect to different patterns of motor unit loss. Neural Plasticity 2021;2021:5513224. Published 2021 Jun 22. doi:10.1155/2021/5513224.
Johnston, J.A., Formicone, G., Hamm, T.M., Santello, M., 2010. Assessment of across-muscle coherence using multi-unit vs. single-unit recordings. Exp. Brain Res. 207 (3–4), 269–282.
Kernell, D., 1965. The limits of firing frequency in cat lumbosacral motoneurons possessing different time course of afterhyperpolarization. Acta Physiol. Scand. 65 (1–2), 87–100.
Kernell, D., 1979. Rhythmic properties of motoneurons innervating muscle fibers of different speed in m. gastrocnemius medialis of the cat. Brain Res. 160 (1), 159–162.
Kernell, D., Ducati, A., Sjöholm, H., 1975. Properties of motor units in the first deep lumbrical muscle of the cat's foot. Brain Res. 98 (1), 37–55.
Krutki, P., Celichowski, J., Łochyński, D., Pogrzebna, M., Mrówczyński, W., 2006. Interspecies differences of motor units properties in the medial gastrocnemius muscle of cat and rat. Arch. Ital. Biol. 144 (1), 11–23.
Krutki, P., Hałuszka, A., Mrówczyński, W., Gardiner, P.F., Celichowski, J., 2015. Adaptations of motoneuron properties to chronic compensatory muscle overload. J. Neurophysiol. 113 (7), 2769–2777.
Kryściak, K., Celichowski, J., Krutki, P., Raikova, R., Drzymała-Celichowska, H., 2019. Factors contributing to sag in unfused tetanic contractions of fast motor units in rat medial gastrocnemius. J. Electromyogr. Kinesiol. 44, 70–77. https://doi.org/10.1016/j.jelekin.2018.11.011.
Kryściak, K., Smith, I.C., Drzymała-Celichowska, H., Celichowski, J., 2020. Initial force production before sag is enhanced by prior contraction followed by a 3-minute rest period in fast motor units of the rat medial gastrocnemius. J. Electromyogr. Kinesiol. 53, 102429 https://doi.org/10.1016/j.jelekin.2020.102429.
Macefield, V.G., Gandevia, S.C., Bigland-Ritchie, B., Gorman, R.B., Burke, D., 1993. The firing rates of human motoneurones voluntarily activated in the absence of muscle afferent feedback. J. Physiol. 471, 429–443. https://doi.org/10.1113/jphysiol.1993.sp019908.
Milner-Brown, H.S., Stein, R.B., Yemm, R., 1973. Changes in firing rate of human motor units during linearly changing voluntary contractions. J. Physiol. 230 (2), 371–390.
Moritz, C.T., Barry, B.K., Pascoe, M.A., Enoka, R.M., 2005. Discharge rate variability influences the variation in force fluctuations across the working range of a hand muscle. J. Neurophysiol. 93 (5), 2449–2459.
Nagamori, A., Laine, C.M., Loeb, G.E., Valero-Cuevas, F.J., 2021. Force variability is mostly not motor noise: theoretical implications for motor control. PLoS Comput. Biol. 17 (3), e1008707.
Negro, F., Orizio, C., 2017. Robust estimation of average twitch contraction forces of populations of motor units in humans. J. Electromyogr. Kinesiol. 37, 132–140.
Negro, F., Yavuz, Ş.U., Farina, D., 2014. Limitations of the spike-triggered averaging for estimating motor unit twitch force: a theoretical analysis. PLoS One 25.
Nordstrom, M.A., Miles, T.S., Veale, J.L., 1989. Effect of motor unit firing pattern on twitches obtained by spike-triggered averaging. Muscle Nerve 12 (7), 556–567.
Petersen, E., Rostalski, P., 2019. A comprehensive mathematical model of motor unit pool organization, surface electromyography, and force generation. Front. Physiol. 10, 176. https://doi.org/10.3389/fphys.2019.00176. Published 2019 Mar 8.
Piotrkiewicz, M., 1982. The main features of isometric force generation process in skeletal muscle. Biocyber Biomed Eng. 2, 45–64.
Piotrkiewicz, M., Celichowski, J., 2007. Tetanic potentiation in motor units of rat medial gastrocnemius. Acta Neurobiol. Exp. (Wars) 67 (1), 35–42.
Piotrkiewicz, M., Miller-Larsson, A, Grottel, K., Celichowski, J., 1986. Tetanic potentiation in rat motor units. Fourth Mediterranean Conference on Medical and Biological Engineering: MECOMBE. 1986;IX: 9–12.
Potvin, J.R., Fuglevand, A.J., 2017. A motor unit-based model of muscle fatigue. PLoS Comput. Biol. 13 (6), e1005581.
Powers, R.K., Binder, M.D., 2001. Input-output functions of mammalian motoneurons. Rev. Physiol. Biochem. Pharmacol. 143, 137–263.
Raikova, R.T., Aladjov, H.T., 2002. Hierarchical genetic algorithm versus static optimization-investigation of elbow flexion and extension movements. J. Biomech. 35 (8), 1123–1135.
Raikova, R., Celichowski, J., Pogrzebna, M., Aladjov, H., Krutki, P., 2007a. Modeling of summation of individual twitches into unfused tetanus for various types of rat motor units. J. Electromyogr. Kinesiol. 17 (2), 121–130.
Raikova, R., Krutki, P., Aladjov, H., Celichowski, J., 2007b. Variability of the twitch parameters of the rat medial gastrocnemius motor units-experimental and modeling study. Comput. Biol. Med. 37 (11), 1572–1581.
Raikova, R., Pogrzebna, M., Drzymała, H., Celichowski, J., Aladjov, H., 2008. Variability of successive contractions subtracted from unfused tetanus of fast and slow motor units. J. Electromyogr. Kinesiol. 18 (5), 741–751.
Raikova, R., Aladjov, H., Celichowski, J., Krutki, P., 2013. An approach for simulation of the muscle force modeling it by summation of motor unit contraction forces. Comput. Math. Methods Med. 625427, 2013.
Raikova, R., Aladjov, H., Krutki, P., Celichowski, J., 2016a. Estimation of the error between experimental tetanic force curves of MUs of rat medial gastrocnemius muscle and their models by summation of equal successive contractions. Comput. Methods Biomech. Biomed. Eng. 19 (7), 763–770.
Raikova, R., Krutki, P., Celichowski, J., 2016b. A general mathematical algorithm for predicting the course of unfused tetanic contractions of motor units in rat muscle. PLoS One 11 (9), e0162385.
Raikova, R., Celichowski, J., Angelova, S., Krutki, P., 2018. A model of the rat medial gastrocnemius muscle based on inputs to motoneurons and on an algorithm for prediction of the motor unit force. J. Neurophysiol. 120 (4), 1973–1987.
Raikova, R., Krasteva, V., Krutki, P., Drzymała-Celichowska, H., Kryściak, K., Celichowski, J., 2021. Effect of synchronization of firings of different motor unit types on the force variability in a model of the rat medial gastrocnemius muscle. PLoS Comput. Biol. 17 (4), e1008282.
Rakoczy J, Kryściak K, Drzymała-Celichowska H, Raikova R, Celichowski J. Biomechanical conditioning of the motor unit transitory force decrease following a reduction in stimulation rate. BMC Sports Sci Med Rehabil. 2020;12:60. Published 2020 Sep 29. doi:10.1186/s13102-020-00208-6.
Roatta, S., Arendt-Nielsen, L., Farina, D., 2008. Sympathetic-induced changes in discharge rate and spike-triggered average twitch torque of low-threshold motor units in humans. J. Physiol. 586 (22), 5561–5574.
Rohlén, R., Raikova, R., Stålberg, E., Grönlund, C., 2022. Estimation of contractile parameters of successive twitches in unfused tetanic contractions of single motor units – A proof-of-concept study using ultrafast ultrasound imaging in vivo. J. Electromyogr. Kinesiol. 67, 102705.
Sanchez, G.N., Sinha, S., Liske, H., Chen, X., Nguyen, V., Delp, S.L., Schnitzer, M.J., 2015. In vivo imaging of human sarcomere twitch dynamics in individual motor units. Neuron 88 (6), 1109–1120.
Sandercock, T.G., 2000. Nonlinear summation of force in cat soleus muscle results primarily from stretch of the common-elastic elements. J. Appl. Physiol. 89 (6), 2206–2214.
Sandercock, T.G., 2003. Nonlinear summation of force in cat tibialis anterior: a muscle with intrafascicularly terminating fibers. J. Appl. Physiol. 94 (5), 1955–1963.
Santello, M., Fuglevand, A.J., 2004. Role of across-muscle motor unit synchrony for the coordination of forces. Exp. Brain Res. 159 (4), 501–508.
Stein, R.B., Parmiggiani, F., 1979. Optimal motor patterns for activating mammalian muscle. Brain Res. 175 (2), 372–376.
Thomas, C.K., Ross, B.H., Calancie, B., 1987. Human motor-unit recruitment during isometric contractions and repeated dynamic movements. J. Neurophysiol. 57 (1), 311–324.
Watanabe, R.N., Magalhães, F.H., Elias, L.A., Chaud, V.M., Mello, E.M., Kohn, A.F., 2013. Influences of premotoneuronal command statistics on the scaling of motor output variability during isometric plantar flexion. J. Neurophysiol. 110 (11), 2592–2606. https://doi.org/10.1152/jn.00073.2013.
Westergaard, R.H., De Luca, C.J., 2001. Motor control of low-threshold motor units in the human trapezius muscle. J. Neurophysiol. 85 (4), 1777–1781.
Williams, E.R., Baker, S.N., 2009. Circuits generating corticomuscular coherence investigated using a biophysically based computational model I. Descending systems. J Neurophysiol. 101 (1), 31–41. https://doi.org/10.1152/jn.90362.2008.
Yao, W., Fuglevand, R.J., Enoka, R.M., 2000. Motor-unit synchronization increases EMG amplitude and decreases force steadiness of simulated contractions. J. Neurophysiol. 83 (1), 441–452.
Zajac, F., 1989. Muscle and tendon: properties, models, scaling, and application to biomechanics and motor control. CRC Crit. Rev Biomed Eng. 17 (4), 359–511.
Zengel, J.E., Reid, S.A., Sypert, G.W., Munson, J.B., 1985. Membrane electrical properties and prediction of motor-unit type of cat medial gastrocnemius motoneurons in the cat. J. Neurophysiol. 53 (5), 1323–1344.
Zero, A.M., Kirk, E.A., Rice, C.L., 2022. Firing rate trajectories of human motor units during activity-dependent muscle potentiation. J. Appl. Physiol. 132 (2), 402–412.